ANALYSIS AND TESTING OF A DAMPING TREATMENT FOR A MULTI-COMPONENT SPACE STRUCTURE

Eric M. Austin and Conor D. Johnson
CSA Engineering, Inc.
Palo Alto, California

Laurence S. Gittleson
Lockheed Missiles and Space Company, Inc.
Sunnyvale, California

ABSTRACT

A large space structure required at least 1% viscous damping for each of its four lowest global modes to reduce vibration response. Due to the complexity of the problem, two of the three components in the system were represented only by stiffness and mass matrices at a reduced set of points. The third component was represented by a finite element model. Damping designs were produced and their performance predicted by computing system-level modal strain energy using both the finite element model and the condensed stiffness matrices. The chosen design produced the required damping with less than 0.2% added weight.

1. Problem Description

This paper summarizes joint work between Lockheed Missiles and Space Company, Inc. (LMSC), and CSA Engineering to design, implement, and test a space-qualified add-on damping treatment for a multi-component space structure. The damping treatment was designed for a cylindrical, barrel-like portion of a structure that is connected to two other larger, more complex structural components. Due to modeling and other interface considerations, only a finite element model (MSC/NASTRAN) of the main section was available for analysis. The remaining subcomponents of the structure were provided in the form of mass and stiffness matrices represented at a reduced set of points in the condensed structures.

The modes of interest for the structure were the first four; the first two being the most critical. These modes occurred in two pairs: the first pair at approximately 16 Hz and the second at 23 Hz. The goal was to increase the system-level viscous damping in both pairs of modes to at least one percent. There was a severe restriction on added weight for the structure, and the main section had many areas which were inaccessible due to proximity of surrounding structure.

2. Analysis Techniques

The system analyses were performed by integrating the main structure and two substructures into a full system model. The three components of the system model are shown schematically in Figure 1. The process of integrating the condensed matrices with those of the finite element model was as follows. All of the operations were done within MSC/NASTRAN using Direct Matrix Abstract Programing (DMAP). Substructure 1 was condensed down to 44 points scattered throughout the structure. There were a total of 129 nonconstrained degrees of freedom (DOF's) among these points, and there were six attachment points between the main finite element model and the first substructure. Given the relationship between the DOF's in the matrices and the attachment points to the finite element model, the inclusion process started by defining GRID points for each of the 38 internal points in the condensed structure. The remaining six points correspond to the attachment points, and were already included as GRID points in the finite element model. A partition vector was then created for the substructure based on sets defined in the MSC/NASTRAN input whose members were the connection and "dummy" GRID points. The partition vector was used to insert the outside mass and stiffness values into the global mass and stiffness matrices. Finally, a MERGE command was done to integrate these matrices in to the system matrices. A similar procedure was followed for the Substructure 2.

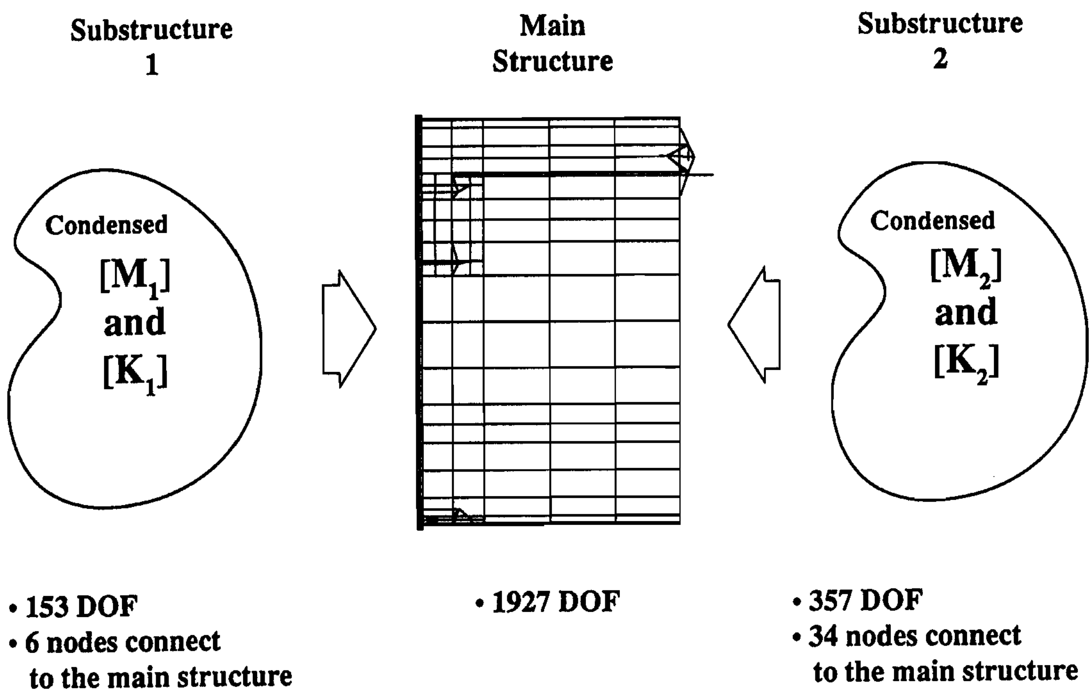

Figure 1. Schematic view of system finite element model

To make predictions of the system-level damping, it was necessary to have knowledge of the system-level strain energy for the modes of interest. NASTRAN will calculate the strain energy for any or all of the model's structural elements. However, the substructures' matrices contain no structural elements *per se*. A method of correctly extracting the strain energy from the missing parts of the structure was therefore required. The strain energy was obtained by performing the following triple-product of the stiffness matrix and partitioned eigenvector for the two condensed portions of the system model.

$$(Strain\ \ Energy)_i = \frac{1}{2}\{\phi_i\}^T[K]\{\phi_i\} \tag{1}$$

where

$\{\phi_i\}$ = component eigenvector of mode "i" partitioned out of the system eigenvector

$[K]$ = component stiffness matrix

	Substructure		
Mode	1	2	Main
1	2.2%	25.1%	72.7%
2	2.4%	26.2%	71.4%
3	21.1%	59.0%	20.0%
4	22.8%	58.0%	19.2%

Table 1. Distribution of modal strain energy in the system for the first four modes

The modal strain energy (MSE) was printed out for each of the substructures in the form of vectors with lengths equal to the number of eigenvectors extracted in the analysis. The system-level MSE was found by simply adding the absolute strain energies of the three components. From this, the percentage of MSE in any particular set of elements could be found. This technique was checked for accuracy on a test model.

Table 1 gives the percentage of strain energy predicted for the three components of the undamped system model. The task of obtaining 1% viscous damping (2% structural) in Modes 3 and 4 is formidable since the structure on which a damping treatment can be applied only has 20% of the system-level modal strain energy for these modes. The predicted mode shapes of the modes of interest are shown in Figure 2. Since the mode shapes are predominantly global, the modal strain energy is predictably well distributed.

First mode pair
~ 16 Hz

Second mode pair
~ 23 Hz

Figure 2. Lowest two mode pairs predicted by the baseline finite element model

3. Candidate Damping Designs

Past experience with similar cylindrical structures has shown that high damping levels, on the order of 10% viscous, could be achieved if the main structure were integrally damped, i.e., the panel sections were made of sandwiched viscoelastic material construction. However, since the structure already existed, this strategy could not be implemented. An add-on treatment of this type was also out of the question due to the large amount of added weight that would have resulted.

The weight-efficient alternative to a full-coverage constrained-layer treatment is to apply damping treatments selectively to structural members containing high MSE in the modes of interest. Analysis showed that the stiffening rings were good candidates. Of these rings, Ring 1 was chosen for detailed study; it had the best combination of accessibility and modal strain energy. Figure 3 shows the undeformed finite element of the main structure. Ring 1 has been refined to allow for modeling of candidate damping treatments. Even though this ring was accessible, there were some tight space limitations on the inner and outer surfaces. Figure 4 shows the cross section of the ring and the envelope for the damping treatment.

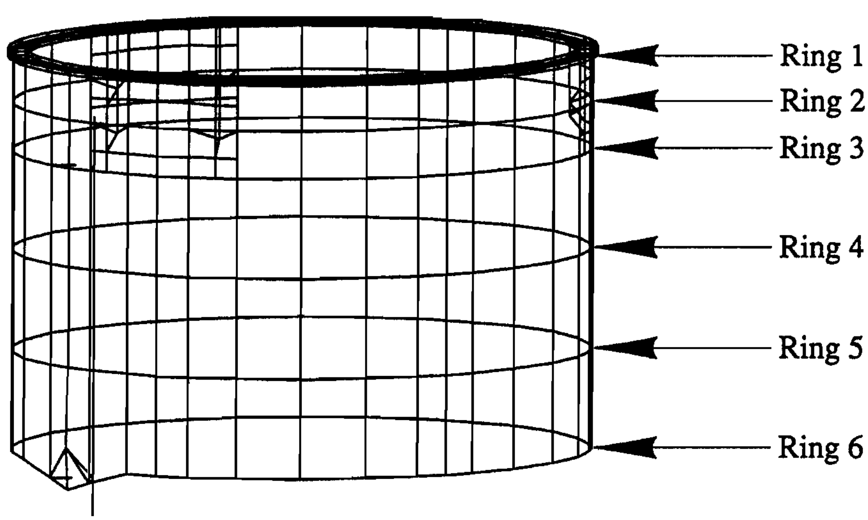

Figure 3. Undeformed finite element model of the main structure

Throughout the iterative design processes, the designs were also driven by factors other than maximum damping. Ease of application was one, since disassembly of the actual article was not possible. Another factor, as shown in Figure 4, was that the outer flanges of Ring 1 were riveted to an inner C-section every few inches. The height of the rivet heads was roughly 0.050 inches.

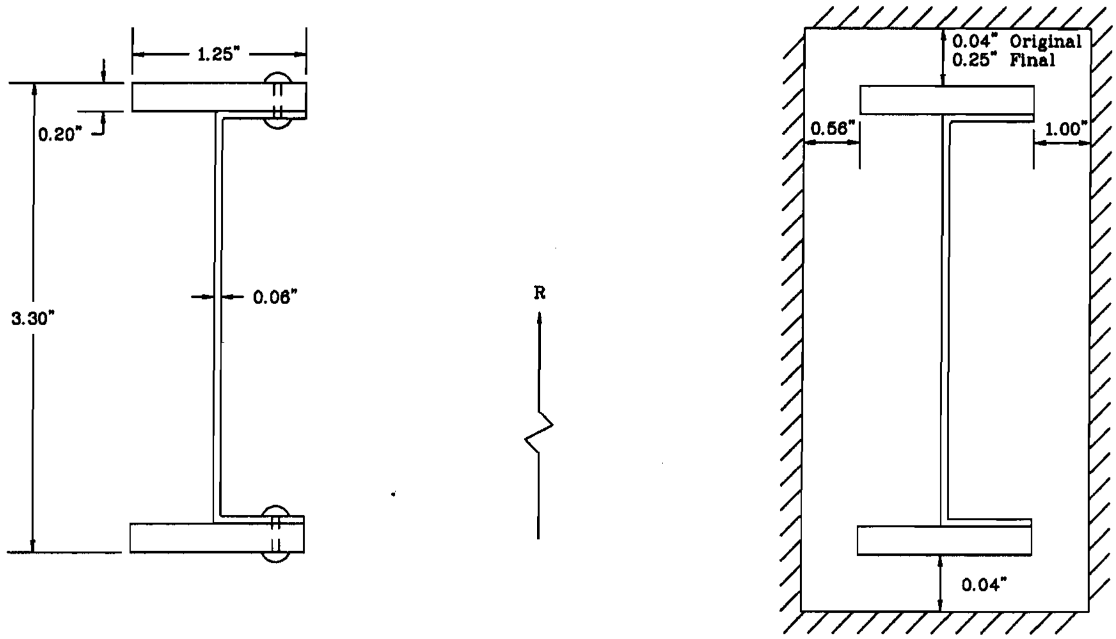

Nominal Dimensions

Envelope Allowed for Damping Treatment

Figure 4. Cross section of Ring 1 with the original space restrictions

Three types of add-on passive damping treatments were investigated: tuned-mass dampers, damped links, and constrained-layer damping. Tuned-mass dampers were ruled out mainly because of the practical problems of tuning and maintaining the devices for a space application. Also, the nature of the mode shapes and the fact that there were two pairs of closely spaced modes meant that tuned-mass dampers were not a good candidate solution for this problem. Link dampers were not a viable solution since there are not any accessible locations of the structure having large relative motions. The remaining choice was some type of constrained-layer treatment.

Many types of constrained-layer treatments were evaluated. Since the target modes shapes were simple, all of the preliminary designs were evaluated on a model of one quarter of Ring 1 with symmetric boundary conditions. All of the early treatments sought to use the relatively large clearances, 0.56 and 1.0 inches, on the front and back sides of the ring, as shown in Figure 4. Some candidate solutions are shown in Figure 5. Within the original space restrictions, none of the candidate solutions was found to produce the required damping, but the treatments with the constrained-layer treatment on the outer rim of the ring were the most promising.

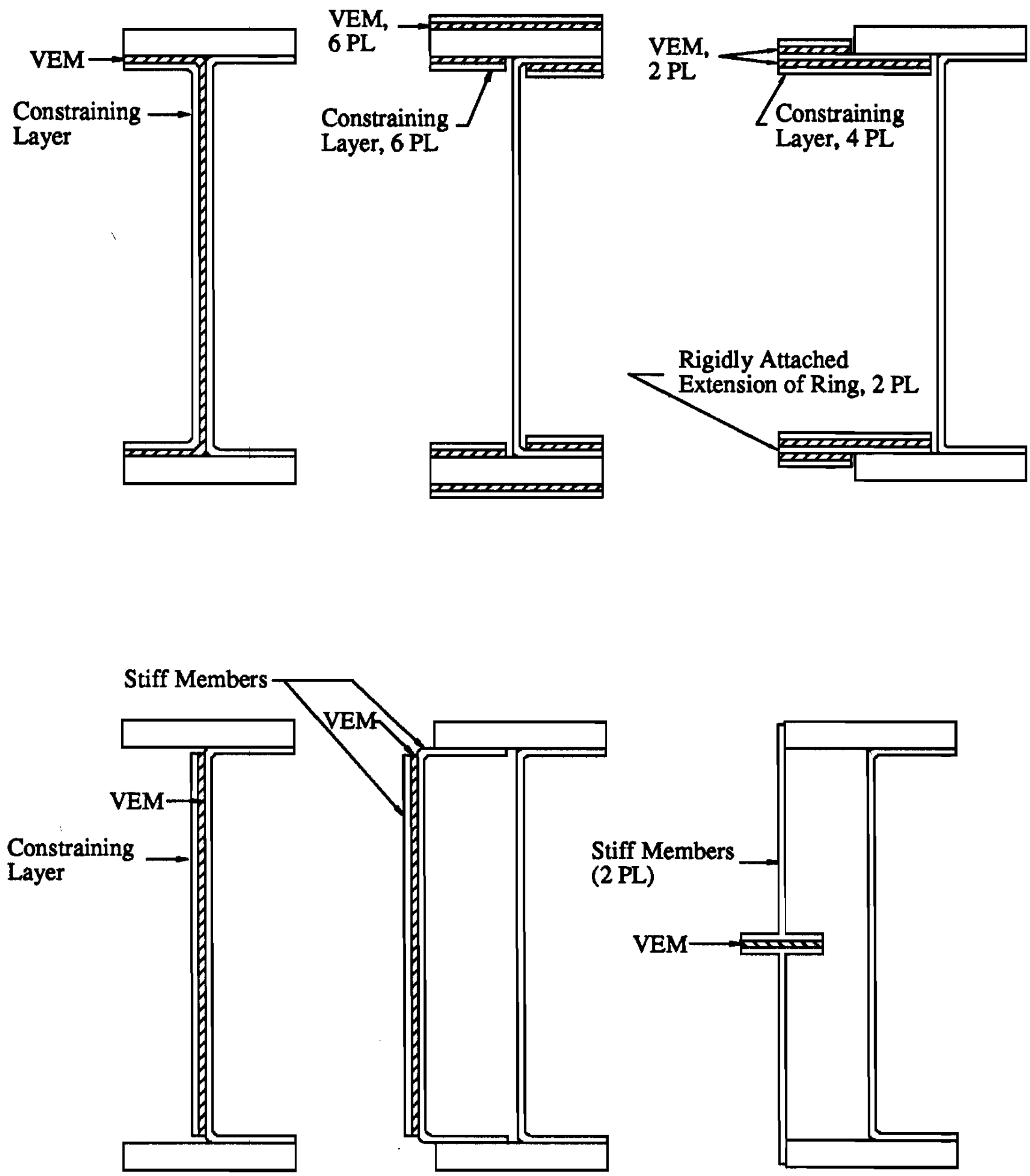

Figure 5. Candidate add-on damping treatments for Ring 1

At this point, these preliminary results were presented for review. The original clearance envelope was based on worst-case assumptions of adjoining structures moving out of phase with respect to each other. After reanalysis of these conservative restrictions, Lockheed decided to increase the allowable space on the outer surface of the ring from 0.040 to 0.25 inches. This allowed for a much stiffer constraining layer on the outer surface of the ring. The eventual recommended treatment consisted of 0.060 inches of 3M's ISD 110 and a stiff, 0.19-inch-thick graphite-epoxy constraining layer. Analysis showed that a three-piece constraining layer could be used.

ISD 110 was chosen because its shear modulus, 900 psi, was near optimum for this application and its loss factor, 1.4, was outstanding. A simple free-free beam was fabricated to verify the VEM properties at the frequency and temperature (room temperature) of the application.* Since ISD 110 is not self-adhesive at room temperature, 3M recommends either an epoxy or heat treating to adhere the VEM to the base structure. Beams using both methods were built. From a modal test of the beam, the shear modulus and loss factor were inferred using 6th-order theory.** The shear modulus was close to the expected value, but the loss factor was roughly 60% low.

Faced with lowering the system damping predictions by 60%, an alternate viscoelastic material had to be sought. The revised design called for 0.090 inches of 3M's Y4945 acrylic foam tape. This material had a shear modulus lower than the optimum, but its loss factor was an excellent 1.1. The free-free beam tests were repeated, and the material properties were confirmed. Additional qualification tests were performed by the manufacturers of the structure. These tests, tailored to this specific mission, included outgassing, life, humidity, and flammability. The VEM was judged satisfactory in all respects except outgassing. The exposed edges of the material were subsequently coated to prevent any possible harmful effects from outgassing.

The choice of Y4945 had two notable side benefits: 1) it is self-adhesive and 2) two 0.045-inch-thick layers would easily clear the rivet heads. During application, the first 0.045-inch layer was applied over the rivet heads, leaving a visible bump. A tool best described as a "cookie cutter" was then used to remove the VEM in the local area of the rivets. After the second layer of VEM was applied, no discernable bump existed over the rivet heads.

*This work pre-dates use of the direct complex modulus testing now in use at CSA.

**Rao, D.K., "Frequency and Loss Factors of Sandwich Beams Under Various Boundary Conditions," Journal of Mechanical Engineering Science, No. 20, Vol. 8, 1978.

4. Test Confirmation

A modal test was instituted to verify the effectiveness of the damping treatment. The treatment applied to the test article differed from the recommendation only in that the constraining layer was 0.25-inch-thick steel instead of 0.19-inch-thick graphite-epoxy. This variation was due to the tight test schedule. The system was tested in both damped and undamped configurations. Table 2 shows a comparison of the frequencies predicted with the undamped NASTRAN model versus the measured frequencies. Note that the damping values were obtained for this "undamped" configuration. These figures represent the inherent damping that exists in spacecraft structures assembled from many components. Damping of this type is not predictable and can only be determined through testing.

	Mode 1	Mode 2	Mode 3	Mode 4
Analysis (% viscous)	16.44 Hz (—)	16.57 Hz (—)	22.10 Hz (—)	23.47 Hz (—)
Test (% viscous)	15.55 Hz (0.32)	16.28 Hz (0.38)	23.31 Hz (0.85)	23.66 Hz (0.60)

Table 2. Predicted and measured frequencies of the untreated structure

The frequencies predicted using the NASTRAN model of the damped system are given in Table 3 along with the test results. The predicted frequencies agreed fairly well with the measured values, generally within 5%. The NASTRAN-predicted damping values shown in Table 3 have been obtained by adding the inherent damping given in Table 2 to the damping prediction from the finite element analysis. It is not clear if this approach is correct since it is not known how the inherent damping is effected by the add-on damping treatment; somewhere between none and all of the damping measured in the "undamped" structure should be added to the analytical predictions.

There are several possible reasons for the over prediction of the damping values, but most would be sources of only small inaccuracies. The most likely candidate is the quality of the system-level mode shapes and, consequently, the distribution of the system-level modal strain energy. Also, it was known that the finite element model was not entirely representative of the actual structure in its test configuration. One major difference was a mass hung on the test structure that participated heavily in the third and fourth modes. This could help explain why the correlation for these modes was not as good as for the first two.

	Mode 1	Mode 2	Mode 3	Mode 4
Analysis (% viscous)	16.64 Hz (2.0)	16.79 Hz (2.2)	22.14 Hz (1.1)	23.48 Hz (0.8)
Test (% viscous)	16.11 Hz (1.9)	17.04 Hz (2.2)	23.37 Hz (1.0)	23.53 Hz (1.0)
Analysis plus inherent damping	(2.3)	(2.6)	(1.9)	(1.4)

Table 3. Predicted and measured frequencies of the damped test structure

5. Conclusion

A lightweight damping treatment was designed successfully for a large, multi-component structure. The modal strain energy was applied to predict system-level damping, even though much of the structure was represented by condensed mass and stiffness matrices. Good agreement was achieved between results of a modal test and the analysis. Faced with obstacles like weight, size, and outgassing, a treatment was designed that met all of the goals at a weight increase of roughly 0.2%. The validation of this damping solution has allowed LMSC to consider integrally designed damping treatments in possible critical situations to minimize the number and magnitude of late-emerging problems.